Investigation of Initial Transmission Effect on Saturable Absorber Optical Performance of Passive Q-Switching Doped Fiber Laser

Zainab Ali Hussein[1*], Abdul- Kareem Mahdi Salih[2]

Abstract

Study of initial transmission effect on performance of saturable absorber material with Er^{+3} doped fiber laser was studied. Cr^{+4}: YAG used as a saturable absorber (SA) in the study. Software computer program buildup in this study for numerical solving of rate equations model by Rung - Kutta –Fehlberg method. The study reported that the maximum optical bleaching, Threshold population inversion density are occurs at earlier buildup time of passive Q-switched, and the pulse reaches high power whenever SA characterized by low initial transmission. The study explains that related to the effect of SA initial transmission on the number density of photons feedback in resonator of laser system.

Key Words: Passive Q-Switched, Er^{+3} Doped Fiber Laser, Optical Bleaching, Instantaneous Transmission.

DOI Number: 10.14704/nq.2021.19.7.NQ21090 **NeuroQuantology 2021; 19(7):103-109**

Introduction

Passive Q-switched technique in lasers widely used in scientific, medicine, military, communications and industrial applications, that is related to many merits, such as simplicity in laser design and low cost (Zhang B., *et al.*, 2018; Zakaria U.N., *et al.* 2018; Zhang K. *et al.* 2018; Qian Q. *et al.*, 2019). It is achieved by employing an saturable absorber element inside the laser cavity (Nady A., *et al.*, 2018). The performance of SA dependent of some factors such as absorption cross section of its ground and the excited levels, its instantaneous absorption and transmission of laser photons, structure, and optical bleaching of SA (Zhang B., *et al.*, 2018; Nady A., *et al.*, 2018; Lee J., *et al.*, 2019). *Cr^{+4}: YAG* has been successfully used as SA fiber doped laser, its is appear excellent convenient with Erbium (Er^{+3}) fiber doped for Passive Q-switched pulse generation (Liu W., *et al.*, 2018). In this work the effect of initial transmission on Cr^{+4}: YAG performance with Er^{+3} doped fiber as active medium (AM) investigated theoretically. *Cr^{+4}: YAG* energy level can be illustrated by figure (1) (Tsunekane M., *et al.*, 2016). While figure (2) (Polman A., *et al.*, 2001) illustrated the Er^{+3} energy levels.

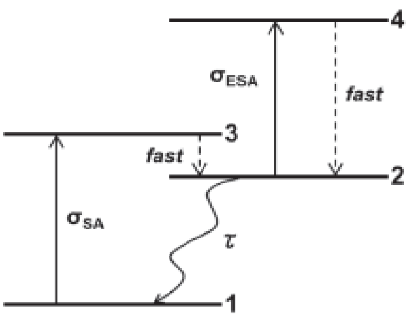

Figure 1. Energy level of *Cr^{+4}: YAG*

Corresponding author: Zainab Ali Hussein
Address: [1*]Physics Department, College of Science, University of Thi–Qar, Thi-Qar, Iraq; [2]Physics Department, College of Science, University of Thi–Qar, Thi-Qar, Iraq.
Relevant conflicts of interest/financial disclosures: The authors declare that the research was conducted in the absence of any commercial or financial relationships that could be construed as a potential conflict of interest.
Received: 15 May 2021 **Accepted:** 19 June 2021

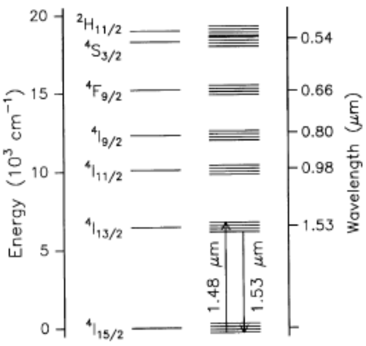

Figure 2. Energy level of Er^{+3}

Theory

Coupled rate equations model (Hussein D. S. *et al.*, 2020) has been used in this study for investigation of SA initial transmission effect on optical performance of SA in Passive Q-switching Er^{+3} doped fiber laser system as the following equations:

$$\frac{d\phi(t)}{dt} = \frac{\phi(t)}{\tau_r}[2\sigma_{am}l_{am}N(t) - 2\sigma_{gs}l_{sa}N_{gs}(t) - 2\sigma_{es}l_{sa}N_{es}(t) - (\ln(\frac{1}{R}) + L_{loss})] \quad (1)$$

$$\frac{dN(t)}{dt} = R_p - \gamma c\sigma_{am}\phi(t)N(t) - \frac{N(t)}{\tau_{am}} \quad (2)$$

$$\frac{dn_{gs}(t)}{dt} = \frac{n_{es}(t)}{\tau_{sa}} - 2\sigma_{gs}l_{sa}\phi(t)n_{gs}(t)/\tau_r \quad (3)$$

$$\frac{dn_{es}(t)}{dt} = -\frac{n_{es}(t)}{\tau_{sa}} + 2\sigma_{gs}l_{sa}\phi(t)n_{gs}(t)/\tau_r \quad (4)$$

Where: ϕ (cm^{-3}) is the photons number density, $\tau_r = 2l_{am}/c$ (s) is the transit time for one round –trip, l_r (cm) is the length of optical cavity, σ_{am} (cm^2) is the active medium emission cross section, c (ms^{-1}) is the light speed, σ_{gs} (cm^{-2}) is the absorption cross section of SA ground-state, l_{am} (cm) is the length of AM, l_{sa} (cm) is the length of SA, n_{gs} (cm^{-3}) is the SA ground state population, N (cm^{-3}) is the active medium population inversion density, n_{es} (cm^{-3}) is the SA exited state population, $R=(R_1R_2)^{1/2}$ is the geometric mean of the cavity, R_1R_2 is the reflectivity of mirrors, l_{loss} is the dissipative optical losses for round –trip. N (cm^{-3}) is the population inversion density, σ_{es} (cm^2) is the absorption cross section of SA excited-state, γ is the population reduction factor equal 1, 2 for 4 levels and 3 level of active medium system respectively, R_p is the optical pumping rate, τ_{sa} (s) is the lifetime of the excited level of SA, τ_{am} (s) is the fluorescence lifetime of the upper laser level. Compared to the fluorescence life of the upper laser level, SA's lifetime in microsecond (Belov M.A., *et al.*, 2015) with the Q-switched laser pulses normally have a very short build-up time, then can be neglect the spontaneous decay in AM and SA, also the pumping rate during pulse generation very longer capering Q-switched laser pulses build-up time (Majli A.S., *et al.*, 2020), then Eq.(2), Eq.(3), and Eq.(4) can be reformulation as the below respectively:

$$\frac{dN(t)}{dt} = -\gamma c\sigma_{am}\phi(t)N(t) \quad (5)$$

$$\frac{dn_{gs}(t)}{dt} = -2\sigma_{gs}l_{sa}\phi(t)n_{gs}(t)/\tau_r \quad (6)$$

$$\frac{dn_{es}(t)}{dt} = 2\sigma_{gs}l_{sa}\phi(t)n_{gs}(t)/\tau_r \quad (7)$$

The density number of photons inside the optical cavity is minimum at the initial time, also most of SA molecules are in the ground state (n_{gs}), then can be regards $n_{gs} \approx n_{so}$, $n_{es} \approx 0$,where ($n_{so} = n_{gs} + n_{es}$) is the total number of SA molecules. The SA absorption activity is also very high at initial time, from Eq.(1) can be consider ($d\phi\ /dt \approx 0$) while cannot consider $\phi(t) = 0$. Then;

$$2\sigma_{am}l_{am}N_o - 2\sigma_{gs}l_{sa}n_{so} - (\ln(\frac{1}{R}) + L_{loss}) = 0 \quad (8)$$

When the pulse passes through the SA, then the spatial variation of the pulse energy per unit aria (E) at any point of the length of SA (at the coordinate along the longitudinal direction of SA) can be expression by(Zhang X. ,*et al.*, 1997):

$$\frac{dE}{dz} = -h\nu n_{so}(1 - \frac{\sigma_{es}}{\sigma_{gs}})[1 - \exp(\frac{-\sigma_{gs}E}{h\nu})] - n_{so}\sigma_{seE} \quad (9)$$

At small energy, the transmission of SA is called small-signal transmission or initial transmission (T_o), at this situation can be regards $\exp(-\frac{\sigma_{gs}E}{h\nu}) \approx (1 - \sigma_{gs}E/h\nu)$ and substituted into Eq. (9), get:

$$\frac{dE}{dz} = [n_{so}\sigma_{gs} - n_{so}\sigma_{es} - n_{so}\sigma_{es}]E$$

eISSN 1303-5150

Given that σ_{gs} greater than σ_{es}. the term which include σ_{es} can be neglected, then:

$$\ln E]_{E_{\min}}^{E_{\max}} = n_{so}\sigma_{gs}\int_0^{l_{sa}} dz$$

The optimization of E_{max} occur when the SA became bleaching to allowed maximum transmission of photons, then can be estimates $E_{\max} \approx \phi_{\max} h\nu$. While the optimization of E_{min} occur when the SA at the high absorption activity, or at small signal transmission of photons, then can be estimated $E_{\min} \approx T_o \phi_{\max} h\nu$.

$$\ln \frac{E_{\max}}{E_{\min}} = \ln \frac{\phi_{\max} h\nu}{T_o \phi_{\max} h\nu} = \ln(\frac{1}{T_o}) = n_{so}\sigma_{gs} l_{sa}$$

$$T_o = \exp(-n_{so}\sigma_{gs} l_{sa}) \quad (10)$$

$$\ln(\frac{1}{T_o^2}) = 2n_{so}\sigma_{gs} l_{sa} \quad (11)$$

Substituted Eq.(11) into Eq. (8), get:

$$N_o = \frac{\ln(\frac{1}{T_o^2}) + (\ln \frac{1}{R}) + L_{loss}}{2\sigma l_{am}} \quad (12)$$

Eq.(12) represent the initial value of population inversion density (N_o)in term of T_0. From eq.(1) , at initial time of pulse can be regards $\frac{d\phi}{dt} \approx 0$, then can be write:

$$Loss(t) = [2\sigma_{gs}\ell_s N_{gs}(t) + 2\sigma_{es}\ell_{sa} N_{es}(t) + (Ln(\frac{1}{R}) + Loss)]/(2\sigma_{am}\ell_{am}) \quad (13)$$

At maximum of ϕ, also from Eq. (1) can be regards ($\frac{d\phi}{dt} \approx 0$), $n_{es} \approx n_{so}$, that mean n_{gs} can be neglected, then can be estimates the threshold population inversion density in term of T_o and β, where ($\frac{\sigma_{es}}{\sigma_{gs}} = \beta$) as the expression:

$$N_{th} = \frac{\beta \ln(\frac{1}{T_o^2}) + \ln(\frac{1}{R}) + L_{loss}}{2\sigma_{am} l_{am}} \quad (14)$$

The instantaneous transmission (time transmission) of a saturable absorber is expressed as follows (Tsunekane M., *et al.*, 2016; Tanaka H., *et al.*, 2020).

$$T(t) = \exp\left[\left\{-\sigma_{gs}(n_{so} - n_{es}(t=0))\exp\left(-\frac{t}{\tau}\right) - \sigma_{es} n_{es}(t=0)\exp\left(-\frac{t}{\tau}\right)\right\}\ell_s\right] \quad (15)$$

The first and second term on the right side represent the instantaneous transmission of ground and excited level of SA respectively.

Results and Discussion

The set of rete equations (1, 5-7) was solved numerically by software computer program preparing in this study using Runga Kutta –Fehlberg method. The data where used reported in the table (1):

Table 1. The input data

parameter	Reference	Parameter	Reference
$l_{am} = 25cm$ $l_r = 300cm$	Savastru D., et al., 2012	$\sigma_{es} = 2.25\times10^{-19} cm^2$	Savastru D., et al., 2013
$\sigma_{am} = 0.575\times10^{-20} cm^2$		$\sigma_{gs} = 8.75\times10^{-19} cm^2$	
$\tau_{am} = 5.545\times10^{-3} s$		$\sigma_{gs} = 8.75\times10^{-19} cm^2$ $\tau_{sa}\ 4.0\times10^{-6} s$	Belov A., et al., 2015
$\gamma = 1$		$R2 = 95\%$	Savastru D., et al., 2012
$\lambda = 1480nm$		$R1 = 90\%$	

Figure (3) shows the synchronization between the passive Q-switching pulse buildup period and the instantaneous transmission when the initial transmission value is 0.137%. At earlier period of pulse generation (0-532ns), it is observed that the number of stimulated photons emitted increases as the instantaneous transmission of SA increases. When the instantaneous transmission reaches its maximum value, the pulse will also reach its maximum value at the same time approximately. The study explains that related to the decreasing of SA absorption until the optical bleaching state occurs at approximately 532 ns, so that the SA has become transparent and allows laser photons to passing through it, and when photons are reflecting, it will increase the stimulated emission that contributes to the rapid construction (buildup) of the pulse and release high energy which stored in AM. In the later period of pulse generation (532-752 ns), it is appear that the number of stimulation emission photons decreasing to low value because the increase of residual absorption activity. The figure also notes that the instantaneous transmission begins to increase after the vanish of optical bleaching state, but this increase does not contribute significantly to the reconstruction of the passive Q-switched pulse. The study explains this to the latent absorption activity state by the excited level ions of the SA. Because of the small value of the absorption cross-section of the excited level compared to the value of the ground level absorption cross-section, the latent absorption activity of excited level is also less ground level and allows for the transmission of photons. The SA will return to the high absorption after time approach to the lifetime of excited level, but this has not been demonstrated due to the large lifetime of the ground level of SA ($\tau_{sa} = 4\times10^{-6} s$) compared to the passive Q-switched pulse generation time (approximately 752 ns) as shown in the figure.

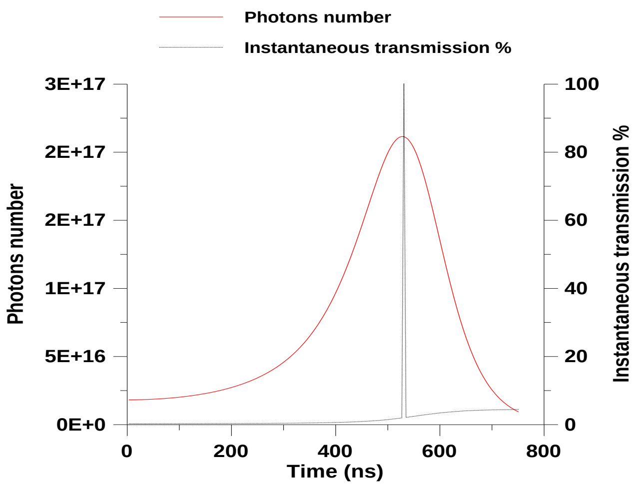

Figure 3. Synchronization maximum photons number of pulse (cm^{-3}) with the optical bleaching time (maximum instantaneous transmission) at T_o=0.137%

Figure (4) shows the synchronization occurrence of the optical bleaching state of SA with the threshold of population inversion density in the AM when T_o=0.137%. In the earlier period of pulse generation time, it is observed that the population inversion density decreases while the instantaneous transmission increasing. When the optical bleaching state of SA taking place (at time approximately 532 ns), the population inversion density reaches threshold value (since the value of the greatest convergence between the value of the photons loss which is represent by the dotted line and the value of the population inversion density represented by the bold), and then becomes normal population. This is explained by that the gradual increase in instantaneous transmission led to a gradual decrease in the value of the ions population density at the excited laser level of the AM. The occurrence of optical bleaching led to a sharp increase in the number of feedback photons return to AM, resulting in a large number of ions transfer from the excited laser level to the ground laser. It should be noted from the figure that the initial population inversion density was 4.608×10^{19} cm $^{-3}$ at the initial transmission value, but its threshold value became 2.777×10^{19} cm^{-3} at the time of maximum optical bleaching case in SA (transmission reaches 100% approximately).

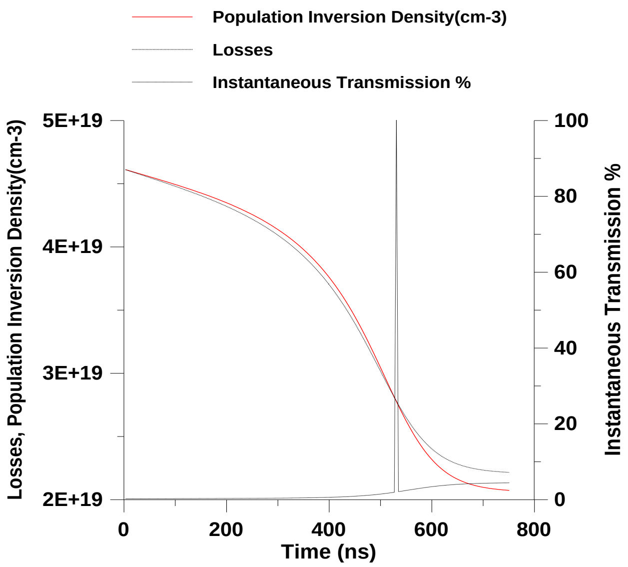

Figure 4. Synchronization threshold population inversion density with the optical bleaching (Max. instantaneous transmission) at T_o=0.137%

Figures (5, 6) represents the case of T_o=0.117% Can be notes that physical behavior and its interpretation are similar to the behavior and its interpretation that being in the figs. (3, 4). But the difference is evident in the values and times of behavior. Figure (5) shows that the pulse is high at 476 ns and is fading at 656 ns approximately. These times are previous than the case of T_o=0.137%. The study interpreting that related to optical bleaching occurred at previous time than the case of T_o=0.137%. Figure (6) also shows that the threshold value of population inversion density is achieved at approximately 476 ns, which is also previous than in the case of T_o=0.137%.

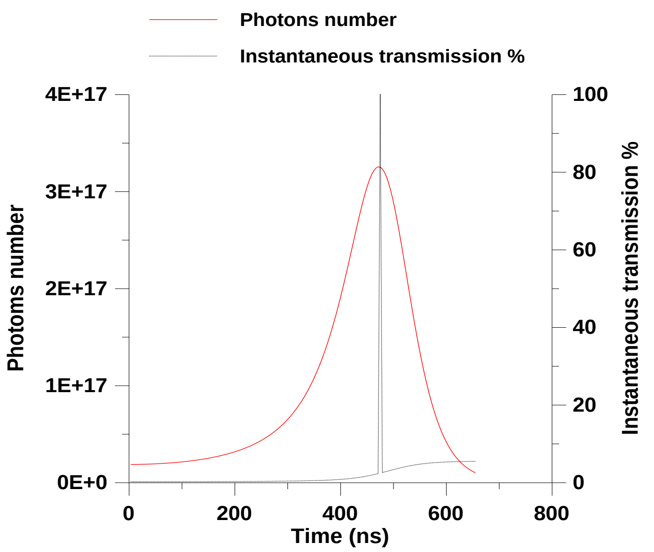

Figure 5. Synchronization maximum photons number with the optical bleaching (maximum instantaneous transmission) at T_o=0.117%

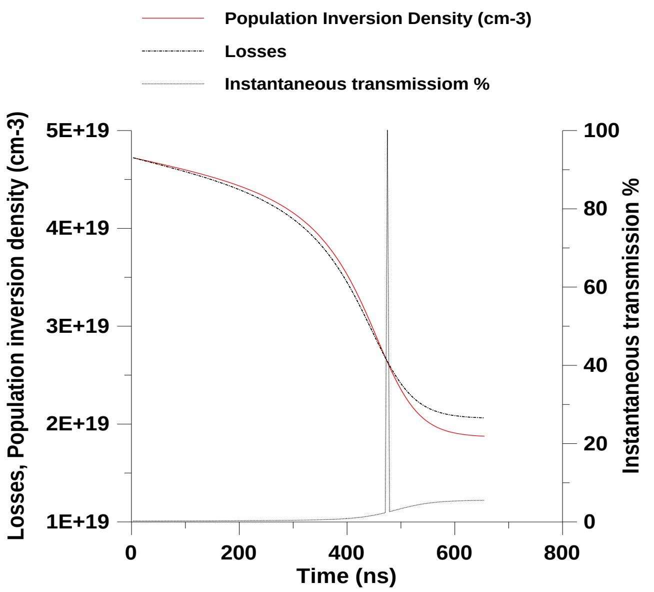

Figure 6. Synchronization threshold population inversion density with the optical bleaching time (Max. instantaneous transmission) at T_o=0.117%

Figures (7, 8) represents the case of T_o=0.097%, they are enhance the results in previous figures of (T_o=0.137%, T_o=0.117%). Can be notes that physical behavior and its interpretation are similar to the behavior and its interpretation that being in the previous figures. Figure (7) shows that the passive Q-switched pulse is high at 424 ns and is fading at 572 ns approximately, These times are previous than the cases of T_o=0.137% and T_o=0.117%. The study interpreting that related to optical bleaching occurred at previous time than the cases of T_o=0.137% and T_o=0.117%. Figure (8) also shows that the threshold value of population inversion density is achieved at 424 ns approximately, this time also previous than in the cases of T_o=0.137% and T_o=0.117%.

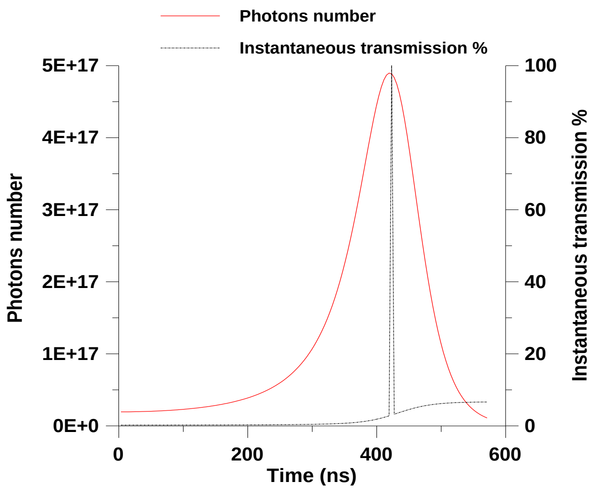

Figure 7. Synchronization maximum photons number of pulse (cm-3) with the optical bleaching time (maximum instantaneous transmission) at T_o=0.097%

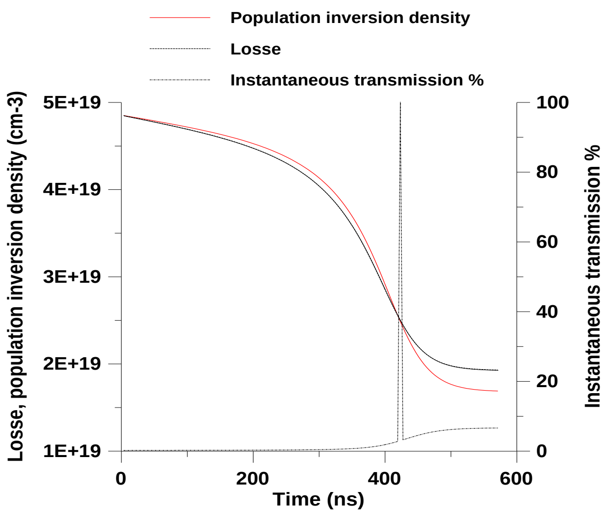

Figure 8. Synchronization threshold population inversion density with the optical bleaching (max. instantaneous transmission) at T_o=0.097%

Figure (9) shows the instantaneous transmission and the optical bleaching states as a function of selected values of T_o, it is observed that the SA becomes incapable of absorption within a very short time period, and then returns to its absorption activity due to the increment of excited level population density because of the ions transferred from the ground level of SA. Because of the absorption cross section of excited level less than of ground level, the residual transmission occurred after the bleaching state related to excited level activity is appear and increases in value with the decreasing of T_o.

Figure (10) illustrates the percentage of instantaneous transmission as a function of T_o, showing that the optical bleaching case occurs at advance time of pulse buildup time whenever the value of T_o is low. The study explains that because of the inverse relationship between the absorption activity of SA and the instantaneous transmission of the photons through SA, that means the low initial transmission indicate to high initial absorption activity of the ground level of SA, that results in an increase in the rate of ions transfer from the ground level to excited level, leading to occur the optical bleaching case at earlier time.

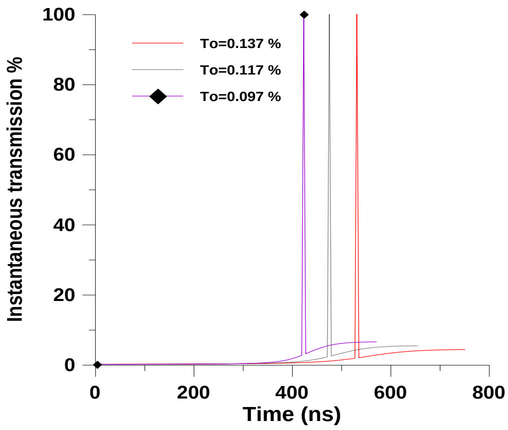

Figure 9. The optical bleaching states as a function of T_o

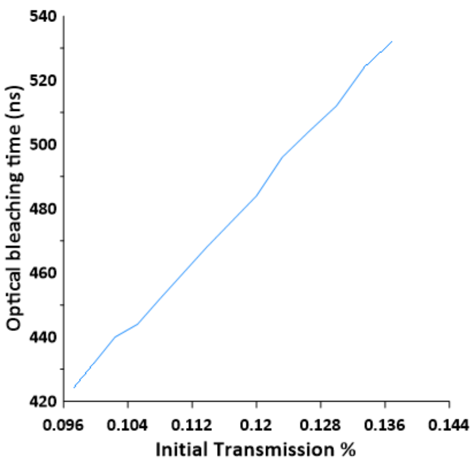

Figure 10. The optical bleaching times as a function of T_o

Conclusion

The maximum optical bleaching, Threshold population inversion density are occurs at earlier buildup time of passive Q-switched, and the pulse reaches high power whenever SA characterized by low initial transmission. Then for improve the performance efficiency of passive Q-switching doped fiber Laser system, it is necessary decreasing the initial transmission of SA.

References

Belov MA, Burov LI, Krylova LG. Influence of the Cr4+: YAG Saturable Absorber Parameters on Output Characteristics of the Nd3+: LSB Laser in Q-Switched Regime. *Nonlinear Phenomena in Complex Systems* 2015; 18(2): 140-148.

Hussein DS, Salih AM. Simulation of fiber length effect on the pulse characteristics of passively Q-switching Yb doped fiber laser. *Test engineering & management* 2020; 83: 22233-22240.

Lee J, Kwon S, Lee JH. Ti 2 AlC-based saturable absorber for passive Q-switching of a fiber laser. *Optical Materials Express* 2019; 9(5): 2057-2066. https://doi.org/10.1364/OME.9.002057

Liu W, Liu M, Han H, Fang S, Teng H, Lei M, Wei Z. Nonlinear optical properties of WSe 2 and MoSe 2 films and their applications in passively Q-switched erbium doped fiber lasers. *Photonics Research* 2018; 6(10): C15-C21. https://doi.org/10.1364/prj.6.000c15

Majli AS, Abdul-Kareem MS. Simulation of Active Medium Emission Cross Section Influence on Passive Q-switching Laser Pulse Characteristics. *NeuroQuantology* 2020; 18(5): 62-66. https://doi.org/10.14704/nq.2020.18.5.NQ20169

Nady A, Latiff AA, Numan A, Ooi CR, Harun SW. Theoretical and experimental studies on a Q-switching operation in an erbium-doped fiber laser using vanadium oxide as saturable absorber. *Laser Physics* 2018; 28(8): 085106. https://doi.org/10.1088/1555-6611/aac715

Polman A. Erbium as a probe of everything? *Physica B: Condensed Matter* 2001; 300(1-4): 78-90.

Qian Q, Kong D, Zhao S, Li G, Cheng X, Wang N, Zang J. Promotion impact of thermal oxidation etching to saturable absorption performance of g-C3N4. *Optics & Laser Technology* 2019; 111: 597-603. https://doi.org/10.1016/j.optlastec.2018.10.041

Savastru D, Miclos S, Lancranjan I. Theoretical Analysis of a Passively Q-Switched Erbium Doped Fiber Laser. *Nonconventional Technologies Review/Revista de Tehnologii Neconventionale* 2012; 16(1): 47–3.

Savastru D, Savastru R, Miclos S, Lancranjan I. Numerical Analysis of Passively Q-switched Er and Yb Doped Fiber Laser. *In PIERS Proceedings*.

Tanaka H, Kränkel C, Kannari F. Transition-metal-doped saturable absorbers for passive Q-switching of visible lasers. *Optical Materials Express* 2020; 10(8): 1827-1842. https://doi.org/10.1364/ome.395893

Tsunekane M, Taira T. Direct measurement of temporal transmission distribution of a saturable absorber in a passively Q-switched laser. *IEEE Journal of Quantum Electronics* 2016; 52(5): 1-7. https://doi.org/10.1109/JQE.2016.2541922

Zakaria UN, Harun SW, Reddy PH, Dutta D, Das S, Dhar A, Yasin M. Q-switched hafnium bismuth erbium-doped fiber laser with bismuth (III) telluride based saturable absorber. *Chalcogenide Letters* 2018; 15(4): 181-186.

Zhang B, Chen Y, Wang P, Wang Y, Liu J, Hu S, Guo J. Direct bleaching of a Cr 4+: YAG saturable absorber in a passively Q-switched Nd: YAG laser. *Applied optics* 2018; 57(16): 4595-4600. http://doi.org/ 10.1364/ao.57.004595

Zhang K, Feng M, Ren Y, Liu F, Chen X, Yang J, Tian J. Q-switched and mode-locked Er-doped fiber laser using PtSe 2 as a saturable absorber. *Photonics Research* 2018; 6(9): 893-899. https://doi.org/10.1364/prj.6.000893

Zhang X, Zhao S, Wang Q, Zhang Q, Sun L, Zhang S. Optimization of Cr/sup 4+/-doped saturable-absorber Q-switched lasers. *IEEE Journal of Quantum Electronics* 1997; 33(12): 2286-2294. https://doi.org/10.1109/3.644112

Wang L. Discussion and analysis on the postgraduate classroom teaching method based on brain science. *NeuroQuantology* 2018; 16(6): 125-131.

eISSN 1303-5150 www.neuroquantology.com